Basin Research

IAS EAGE

Basin Research (2010) **22**, 126–138, doi: 10.1111/j.1365-2117.2009.00440.x

Detrital zircon geochronology and its provenance implications: responses to Jurassic through Neogene basin-range interactions along northern margin of the Tarim Basin, Northwest China

Zhong Li* and Shoutao Peng*,†

*Institute of Geology and Geophysics, Chinese Academy of Sciences, Beijing, China
†Exploration & Production Research Institute, SinoPec, Beijing, China

ABSTRACT

Previously published research from the Kuqa Subbasin along northern margin of the Tarim Basin shows five tectonic-depositional phases from Triassic to Neogene time. In order to reveal additional detailed information on the nature of provenance terrains and tectonic attributes since late Mesozoic time, five typical sandstone samples from Jurassic–Neogene strata were collected for U–Pb dating of detrital zircons. Geochronological constitution of detrital zircons of the Middle Jurassic sample is essentially unimodal and indicates major contributions from the South Tian Shan even Yili–Central Tian Shan, wherein most 370–450 Ma zircons probably resulted from tectonic accretion events between the Yili–Central Tian Shan block and South Tian Shan Ocean during Silurian and Devonian time, with sandstone provenance tectonic attributes of passive continental margin. The Lower Cretaceous sample shows a complicated provenance detrital zircon signature, with new peak ages of 290–330 Ma as well as 370(or 350)–450 Ma showing evident arc orogenic provenance tectonic attribute, probably reflecting a new provenance supply that resulted from denudation process whthin the South Tian Shan and South Tian Shan suture. There are no obvious changes within age probability spectra of detrital zircons between the Cretaceous and early Paleogene samples, which suggests that similar provenance types and basin-range framework continued from Cretaceous to Early Paleogene time. However, unlike the Cretaceous and early Paleogene samples, an age spectra of the Miocene sample is relatively unimodal and similar to that of the Pliocene sample, with peak ages ranging between ~392 and ~458 Ma older than the comparable provenance ages (peak ages about 370–450 Ma) of the Middle Jurassic and Lower Cretaceous samples. Therefore, we conclude that the South Tian Shan was rapidly exhumated and the southern South Tian Shan had become the main source of clastics for the Kuqa Subbasin since the Miocene epoch.

INTRODUCTION

The Tian Shan (Heavenly Mountains) of northwestern China is topographically characterized by higher west and lower east, with a peak elevation of 7000 m. Resulting from multiple accretion and collisions of different blocks in Late Paleozoic time (Coleman, 1989; Windley *et al.*, 1990, 2007; Allen & Zhang, 1992; Carroll *et al.*, 1995), intense intracontinental structural deformation occurred in the Tian Shan and adjacent areas during Mesozoic–Cenozoic, which controlled coeval basin-range evolution and surface processes (Molnar & Tapponier, 1975; Tapponier & Molnar, 1979; Hendrix *et al.*, 1992; Avouac *et al.*, 1993; Burtman *et al.*, 1996; Yin *et al.*, 1998; Allen *et al.*, 1999; Burtman, 2000; Heermance *et al.*, 2007). The Kuqa Subbasin is located within the Tarim basin, in which relatively successive depositional and structural deformation records of Mesozoic–Cenozoic are preserved. Therefore, the Kuqa Subbasin–Tian Shan system is a key tectonic region to study basin-range relationship and continental evolution. Although many advances in structural and sedimentary geology of the Mesozoic–Cenozoic basins adjacent to the Tian Shan have been published, and its tectonic evolution has generally documented (Hendrix *et al.*, 1992; Graham *et al.*, 1993; Lu *et al.*, 1994; Hendrix, 2000; Liu *et al.*, 2000; Li *et al.*, 2003, 2004), the geodynamic attributes

Correspondence: Z. Li, Institute of Geology and Geophysics, Chinese Academy of Sciences, PO Box 9825, Beijing 100029, China. E-mail: lizhong@mail.igcas.ac.cn

and evolution of the Kuqa Subbasin–Tian Shan are still ambiguous. Building upon our recently published data on Jurassic–Neogene depositional systems, this research focuses on depositional responses to Mesozoic–Cenozoic basin-range interactions, with attention on detrital zircon geochronology and its provenance implications, and further explores tectonic controls and detailed processes of the Kuqa Subbasin–Tian Shan system.

TECTONIC UNITS AND REGIONAL GEOLOGY OF THE TIAN SHAN–KUQA SUBBASIN

The Tian Shan is the largest intracontinental orogenic belt in Central Asia, and the Tarim and Junggar basins are located along its south and north sides, respectively (Fig. 1). Previous work suggests that Tian Shan orogenesis terminated in late Paleozoic time (Coleman, 1989; Carroll *et al*., 1990; Sengör *et al*., 1993; Zhou *et al*., 2001), but was subsequently modified by a series of Mesozoic–Cenozoic intracontinental deformation events, probably related to accretion process occurred in the far southern margin of the Eurasian Plate (Dewey *et al*., 1988; Avouac *et al*., 1993). Two late Paleozoic sutures, the North Tian Shan Suture and the South Tian Shan Suture, had been identified according to ophiolite melanges within the Tian Shan area (Allen & Zhang, 1992; Gao *et al*., 1998). Accordingly the Tian Shan and its adjacent area may be divided into five tectonic units from north to south, Junggar basin, North Tian Shan, Yili–Central Tian Shan (Central Tian Shan island arc), South Tian Shan and Tarim basin (Fig. 1a). Some researchers indicated that the North Tian Shan and South Tian Shan all have complicated structural attributes. Generally the North Tian Shan is considered to be a tectonic–lithofacies belt of Devonian–Carboniferous, the Central Tian Shan attributed to an island arc belt with pre-Cambrian basement, and the South Tian Shan may be a tectonic–lithofacies (mélange?) belt of Devonian (?)–Carboniferous age (Fig. 1a).

The Kuqa Subbasin, situated south of the Tian Shan, is an important Mesozoic–Cenozoic tectonic unit in the northern Tarim basin (Jia, 1997). The Kuqa Subbasin and South Tian Shan together constitute a basin-range system (Fig. 1b and c). The Kuqa Subbasin was developed by Mesozoic–Cenozoic depositional records in thickness of 6000–8000 m, which principally show fluviolacustrine and alluvial sedimentary systems.

Paleocurrent measurements from Mesozoic–Cenozoic strata within the northern Kuqa Subbasin are mainly south-directed (Hendrix *et al*., 1992; Graham *et al*., 1993; Hendrix, 2000; Li *et al*., 2004), reflecting tectonic compression and uplift during this time frame. Therefore, a mass of terrestrial detrital materials from the Tian Shan highland were transported and preserved in the Kuqa Subbasin. The relatively continuous depositional records within the northern Kuqa Subbasin therefore presents an excellent opportunity for analyzing basin-range interactions in this intracontinental tectonic setting.

SAMPLE, ANALYTICAL METHODS AND DATA

Along a belt between the Kuqa Subbasin and South Tian Shan, four relatively successive depositional profiles of Mesozoic–Cenozoic strata were investigated with systemic sampling at Wenquan, Kelasu River, Kuqa River and Yangxia (Fig. 1b). For each profile, we had studied depositional records, sandstone framework grain compositions, detrital heavy mineral compositions and whole-rock geochemical compositions (Li *et al*., 2004, 2005), and five tectonic-depositional phases from Lower Triassic to Neogene were primarily outlined.

On the basis of the work mentioned above, five respective sandstone samples were selected from the Kuqa River profile (Table 1, Fig. 6), and their detrital zircons were separated for U–Pb dating in order to further explore tectonic controls and detailed evolutional processes of the late Mesozoic–Cenozoic Kuqa Subbasin–Tian Shan system. This analytical method can be described as follows.

First, detrital heavy minerals were separated from sandstone samples by the standard procedures for mineral separation (Li *et al*., 2004), and then detrital zircons were carefully identified under a binocular microscope. Clean detrital zircons with well-formed crystal shapes were selected and mounted in epoxy adhesive within 1 cm diameter rings and then were polished to yield a smooth flat surface (slice) exposing the interiors of most zircon grains. Cathodoluminescence (CL) images, obtained by a CAMECA SX-50 microprobe (Cameca, France), were used to detect internal textures related to origin and choose potential target sites for U–Pb dating of zircons before analysis.

Laser ablation ICP-MS zircon U–Pb analyses were conducted on an Agilent 7500a ICP-MS (Hewlett–Packard, USA) equipped with a 193 nm laser, housed at the Key Laboratory of Continental Geodynamics, Northwest University in Xi'an, China. Zircon 91500 (Wiedenbeck *et al*., 1995) was used as the standard and the standard silicate glass NISTwas used to optimize the machine: the spot diameter was 30 μm. The detailed analytical technique is described in Yuan *et al*. (2004). The common-Pb correction used the method described by Andersen (2002), since the signal intensity of ^{204}Pb was much lower than the other Pb isotopes and there is a large isobaric interference from Hg. For zircons older than 1000 Ma, ages were calculated from their ^{207}Pb/^{206}Pb ratios, whereas zircon ages younger than 1000 Ma were based on their ^{206}Pb/^{238}U ratios, which provides a more reliable age estimate for these younger grains due to the low content of radioactive Pb and the uncertainties in common lead correction (Sircombe, 1999). Raw count rates for ^{29}Si, ^{204}Pb, ^{206}Pb, ^{207}Pb, ^{208}Pb, ^{232}Th and ^{238}U were collected for age determination. U, Th and Pb concentrations were calibrated using ^{29}Si as an internal

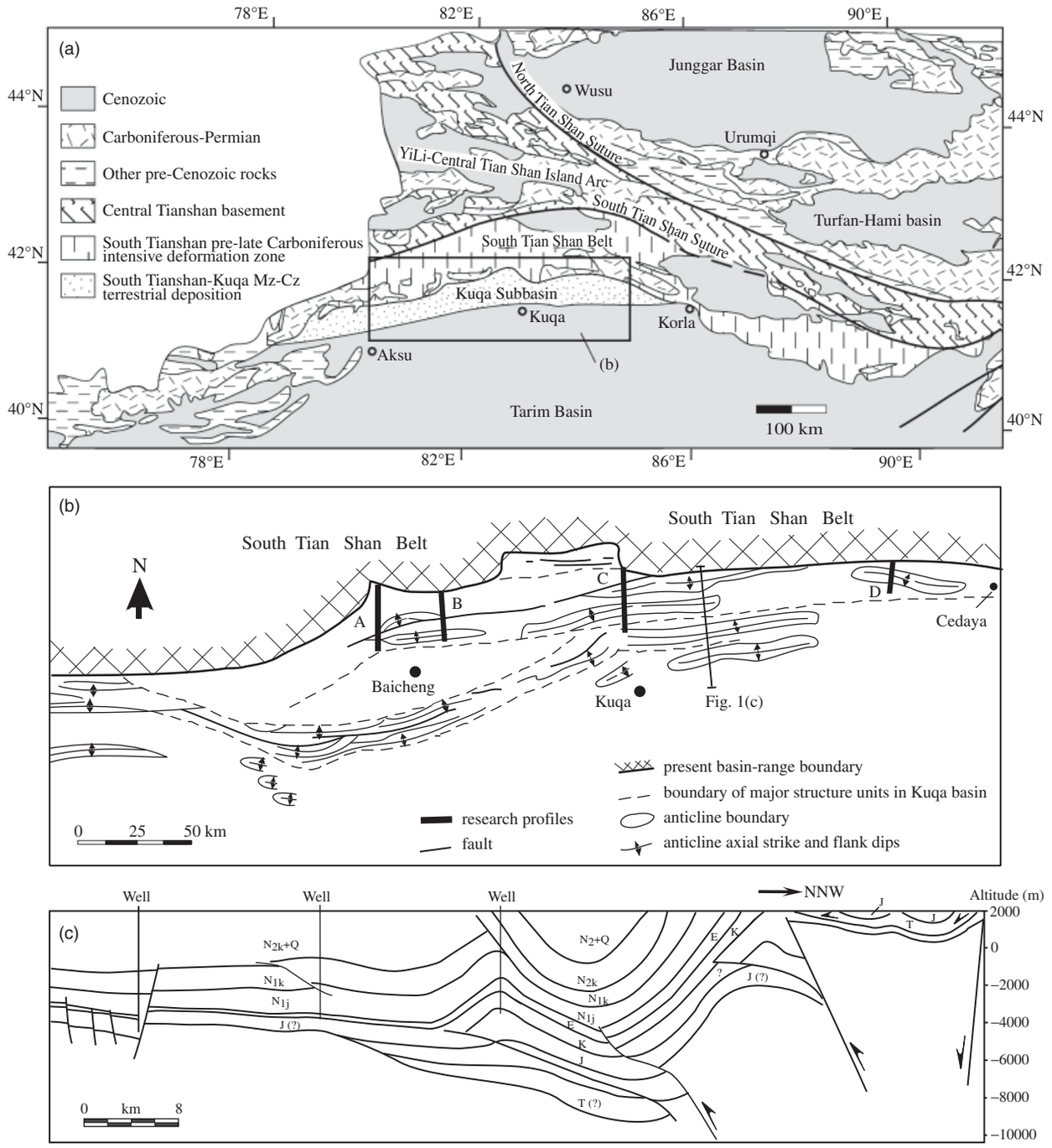

Fig. 1. Tectonic units division in Tian Shan and its adjacent area (compiled from Li *et al.*, 2004). (a) Regional tectonic framework and stratigraphic outcrops of the Tian Shan and adjacent areas, northwest China. (b) Schematic plot showing tectonic framework of the Kuqa Subbasin and the sampling profiles from west to east: A, Wenquan; B, Kelasu River; C, Kuqa River; D, Yangxia. (c) A typical structural cross section interpreted from seismic data across the Kuqa Subbasin, showing fold (wide syncline and narrow anticline) and thrust structures in the interior of the Kuqa Subbasin and coeval normal faults at the present day basin-range boundary. Section location labeled in (b).

calibrant and NIST 610 as reference material. $^{207}Pb/^{206}Pb$ and $^{206}Pb/^{238}U$ ratios were calculated using the GLITTER program version 4.0. Following Ballard *et al.* (2001), measured $^{207}Pb/^{206}Pb$, $^{206}Pb/^{238}U$ and $^{208}Pb/^{232}Th$ ratios in zircon 91500 were averaged over the course of the analytical session and used to calculate correction factors. These correction factors were then applied to each sample to correct for both instrumental mass bias and depth-dependent elemental and isotopic fractionation. The age calculations and plotting of concordia diagrams were made using ISOPLOT (version 3.0) (Ludwig, 2003).

In situ U–Pb dating grains, about 70–90 grains each sample, were selected randomly in each sample slice. Some grains with visible fractures, inclusions and $< 50\,\mu m$ in

Table 1. Distribution of Late Mesozoic-Cenozoic detrital zircon samples in the Kuqa River profile, Kuqa Subbasin

Age	Formation	Sample code	Stratigraphic position	Geographical location via GPS coordinate	Lithology
Pliocene	Kuqa Fm.	DK-N_{2k}-5	Lower part	42°02′03″N 83°05′11″E	Medium-fine sandstone
Miocene	Jidike Fm.	DK-N_{1j}-4	Lower part	42°04′50″N 83°04′52″E	Medium-fine sandstone
Early Paleogene	Kumugeliemu Fm.	DK-E_{km}-4	Bottom part	42°05′10″N 83°05′05″E	Medium-fine sandstone
Early Cretaceous	Yageliemu Fm.	DK-K_{1y}-4	Top part	42°06′37″N 83°08′35″E	Medium-grained sandstone
Middle Jurassic	Qiakemake Fm.	DK-J_{2q}-1	Middle part	42°08′27″N 83°06′25″E	Fine sandstone

diameter were eliminated from analysis. The $^{207}Pb/^{206}Pb$ age is used when the age is >1000 Ma and the $^{206}Pb/^{238}U$ age is used when the age is <1000 Ma, which provides a more reliable age estimate for these younger grains due to the imprecise measurement of ^{207}Pb in young zircons. Those ages with discordance degree $>10\%$ were excluded from analysis. Isotopic ages with errors and related raw data are listed in full as Table A1–A5.

U–Pb GEOCHRONOLOGY OF DETRITAL ZIRCONS

Concordia plots of zircon U–Pb ages for all five samples are shown in Fig. 2, and the corresponding age-probability plots in Fig. 3, using the program of Ludwig (2003). U–Pb geochronology of each sample are described as follow.

Middle Jurassic Qiakemake Formation sample (DK-J_{2q}-1)

A total of 80 zircon grains were measured from the Middle Jurassic sandstone sample collected from the Qiakemake Formation, and 77 effective data points were obtained (Fig. 2). U–Pb ages of 62 detrital zircons range from 366 to 446 Ma, with four zircons ranging from 453 to 476 Ma (Fig. 3e). Most zircons are characterized by high Th/U ratios (0.46–2.48) and oscillatory zones in CL images, indicative of a magmatic origin. One zircon (425 Ma) probably is of metamorphic origin as suggested by its lower Th/U ratio (0.07) and cloudy internal character.

The other zircon U–Pb ages from the Middle Jurassic sandstone sample range from 821 to 3242 Ma and can be divided into three groups, 821–992 Ma (three grains), 1150–1220 Ma (three grains) and 1604–3242 Ma (five grains). The first two age groups suggest relatively determinate tectonic-thermal events. The latter group consists of five extraneous ages. These zircon grains mostly show faint zoning in CL images, suggestive of a metamorphic origin, although two grains of Meso- to Neoproterozoic age are clearly zoned and suggestive of a magmatic origin.

Lower Cretaceous Yageliemu Formation sample (DK-K_{1y}-4)

Seventy-nine zircon grains were random selected and 72 effective U–Pb dates were obtained from the sample of Yageliemu Formation. U–Pb ages range widely from 150 to 2962 Ma. Most ages can be divided into five groups: 150–162 Ma (four grains), 239–266 Ma (four grains), 283–329 Ma (17 grains), 339–427 Ma (27 grains) and 455–467 Ma (three grains). In addition, a relatively small number of old ages were determined from the Early Cretaceous sandstone sample. These include ages of 753–773 Ma (three grains), 865 Ma (one grain), 927–1023 Ma (four grains), 1784 Ma (one grain), 1951 Ma (one grain), 2423–2434 Ma (three grains), 2647–2683 Ma (three grains) and 2962 Ma (one grain) (Figs 2 and 3d).

The zircons that yield dates in the ranges of 150–162 and 239–266 Ma are characterized by high Th/U rations (0.47–1.22) and show distinct oscillatory zones indicative of a magmatic origin. Of the group of zircons dated between 283 and 329 Ma, 93% are attributed to magmatic origin, based on their high Th/U rations and well-zoned internal textures. The other two groups of 339–427 and 455–467 Ma have notable characteristics of high Th/U rations (0.43–1.67) with regular oscillatory zones in CL images, suggestive of a magmatic origin.

Zircons that were separated from Early Cretaceous sandstone and yield old ages are clustered into two groups. The first ranges between 753 and 773 Ma, and the second ranges between 927 and 1023 Ma. Each group contains zircons with both magmatic and metamorphic textures. A third group yielding ages between 1784 and 2962 Ma display faint zoning suggestive of a metamorphic origin.

Lower Paleogene Kumugeliemu Formation sample (DK-E_{km}-4)

Seventy zircon grains were random selected and 66 effective U–Pb dates were obtained from the sample of Kumugeliemu Formation. U–Pb ages from this sample also show a wide range from 240 to 2415 Ma, largely similar to that of the Yageliemu Formation except for the notable absence

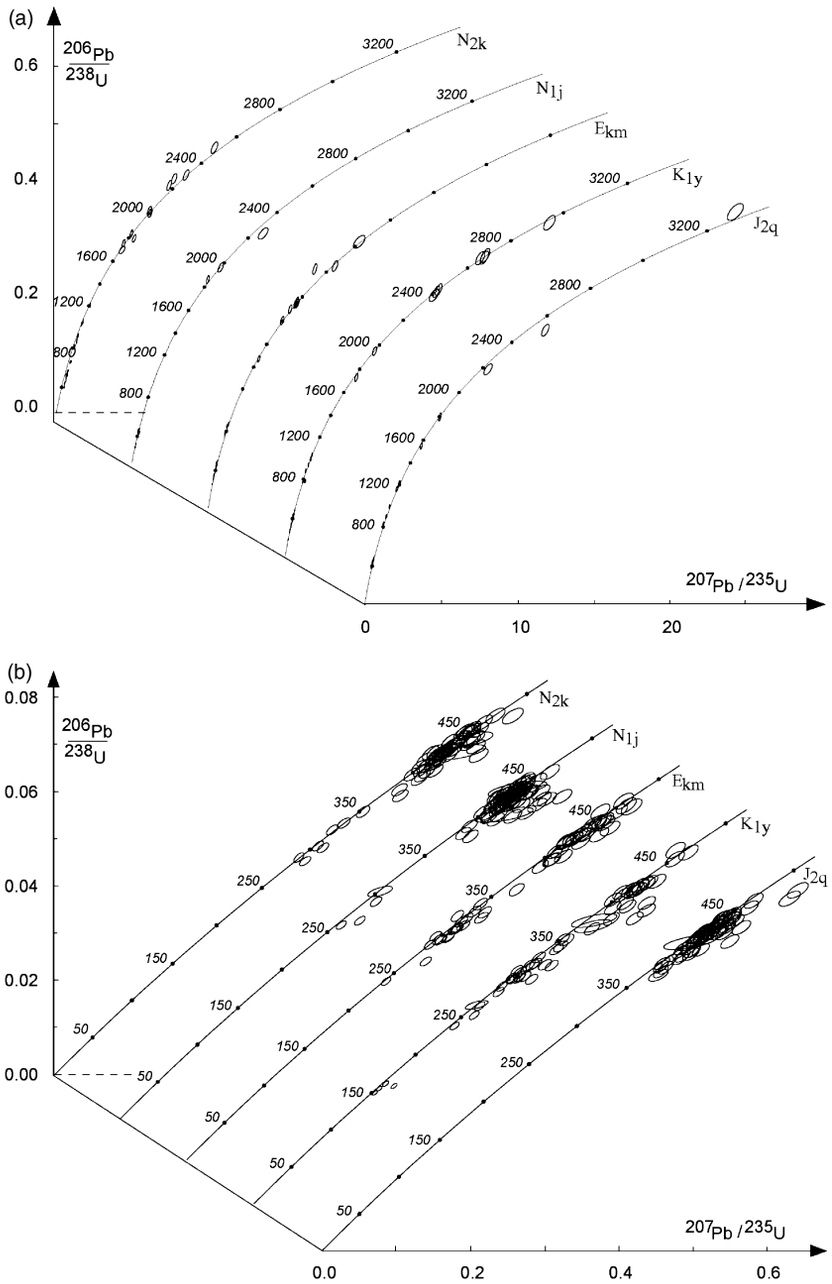

Fig. 2. Concordia plots for detrital zircons from Middle Jurassic–Neogene sandstone samples in Kuqa Subbasin. All ages with discordance degree > 10% were excluded. Errors are shown at 2-sigma level. (a) 0–3700 Ma grains; (b) 0–500 Ma grains. Sample codes referred to Table 1.

of < 165 Ma zircons. Most ages can be divided into four groups: 240–266 Ma (two grains), 288–331 Ma (18 grains), 341–449 Ma (29 grains) and 459–473 Ma (five grains). Several individual or small age clusters are also present, indicating a complicated provenance signature. These include ages of 756–848 Ma (three grains), 1510 Ma (one grain), 1785 Ma (one grain), 1870–1954 Ma (four grains), 2000 Ma (one grain), 2281 Ma (one grain) and 2415 Ma (one grain) (Figs 2 and 3c).

Zircons comprising the age clusters at 240–266 and 288–331 Ma are suggestive of a magmatic origin due to high Th/U rations, ranging from 0.33 to 1.15 (except one grain with 0.03) and elongated euhedral crystals with clear zoning in CL images. The groups of 341–449 and 459–473 Ma, comprising 51.5% of the total grain populations, are also characterized by higher Th/U rations from 0.42 to 1.25 (except one grain with 0.21). However, three grains in the groups of 341–449 Ma display faint internal zoning interpreted to reflect a metamorphic genesis. In addition, the nearly all detrital zircons older than 756 Ma from this sample are attributed to metamorphic origin due to their lower Th/U rations and distinct CL patterns.

Miocene Jidike Formation sample (DK-N_{1j}-4)

Eighty zircon grains were random selected and 77 effective U–Pb dates were obtained from the sandstone sample collected from the Jidike Formation. U–Pb ages mostly range from 401 to 458 Ma (66 grains), with a small number of ages ranging from 260 to 304 Ma (four grains), 1800 Ma

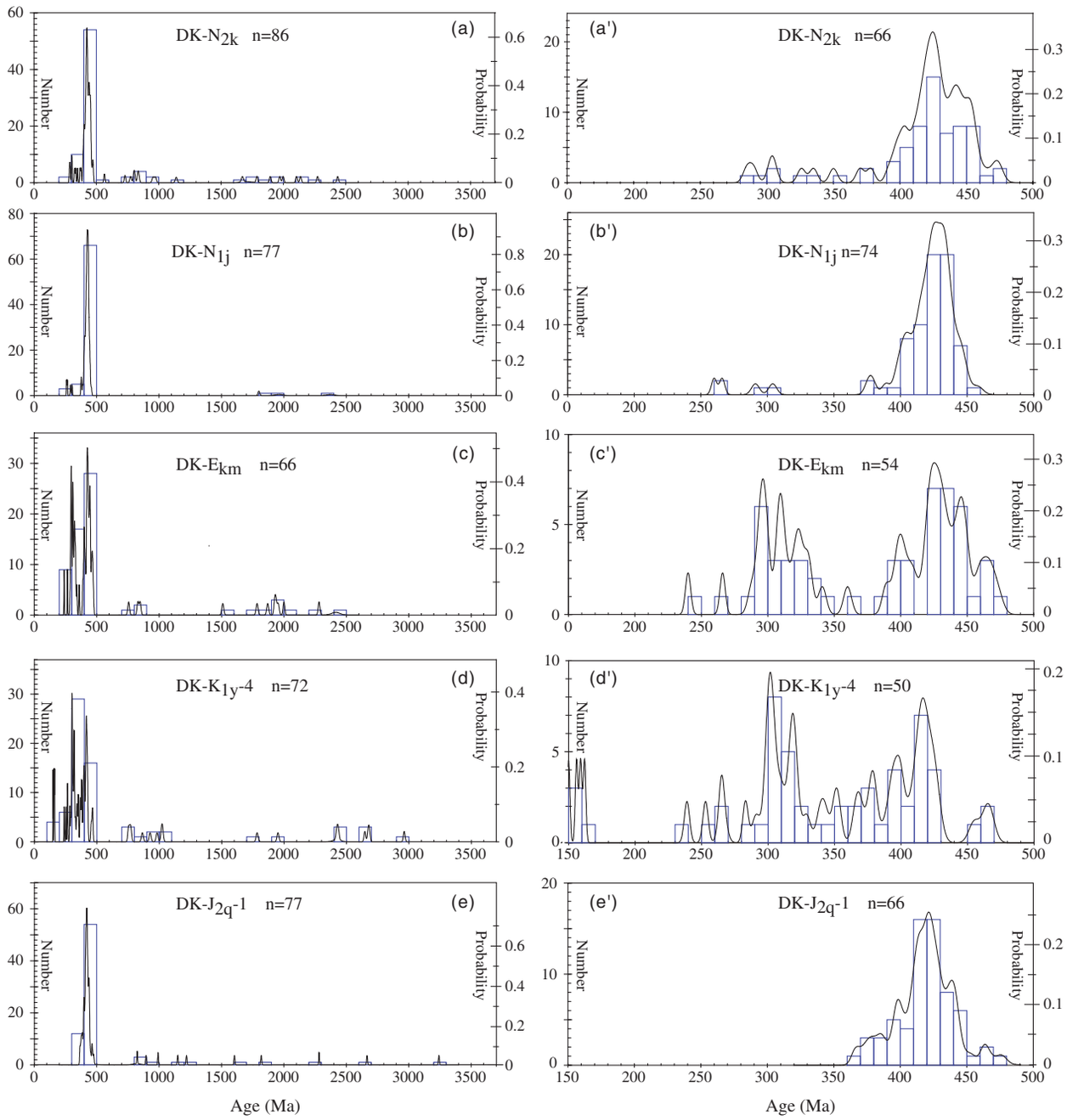

Fig. 3. Probability plots and number histograms of U–Pb ages of detrital zircons from Middle Jurassic–Neogene sandstone samples in Kuqa Subbasin. (a)–(e) 0–3700 Ma grains; (a′)–(e′) 150–500 Ma grains. Sample codes referred to Table 1.

(one grain), 2374 Ma (one grain) and 2374 Ma (one grain) (Figs 2 and 3b). Compared with the sandstone sample of the Kumugeliemu Formation, the detrital zircon age spectra from the Jidike Formation indicate a relatively single provenance constitution.

The group zircons ranging in age from 376 to 458 Ma represents ~91% of the analyzed grain populations. These grains are interpreted to be of magmatic origin due to higher Th/U rations (0.47–1.28) and crystal zonation textures in CL images. However, two grains in the groups of 376–458 Ma show faint crystal texture probably reflective of a metamorphic genesis. In addition, the three zircon grains of Early Proterozoic all show metamorphic genesis with typical fan-shaped zonation or faint zones.

Pliocene Kuqa Formation sample (DK-N_{2k}-5)

Ninety zircon grains were random selected and 86 U–Pb dates were obtained from the sandstone sample from the Kuqa Formation. U–Pb ages mostly range from 392 to 456 Ma (54 grains), with a small number of ages clustered at 285–305 Ma (four grains), 326–350 Ma (three grains),

464–473 Ma (three grains), 730–839 Ma (six grains), 955–974 Ma (two grains), 1671–1788 Ma (three grains), 1894 Ma (one grain), 1971–1998 Ma (two grains), 2105–2137 Ma (two grains), 2274 Ma (one grain) and 2435 Ma (one grain), respectively (Figs 2 and 3a).

Despite the wide age spectra measured from zircons extracted from this sample, the sample is clearly dominated by ages ranging between 370 and 456 Ma, suggesting a provenance broadly similar to that of the Miocene Jidike Formation. The group of 370–456 Ma zircons includes ~66% of the analyzed grains, which, together with the two groups of 285–305 and 326–350 Ma, are mostly attributed to a magmatic origin due to higher Th/U rations (0.90–2.41) and well-zoned crystal textures in CL images. Five grains in the group of 370–456 Ma show faint internal zoning probably indicative of metamorphic genesis.

Compared with the sample of Jidike Formation, notable more dates of pre-Cambrian (Proterozoic) age are present (~21% of the analyzed grain populations) in the sample from the Kuqa Formation. These pre-Cambrian zircons mostly have weak or no internal zoning, suggestive of a metamorphic origin, although one zircon of Neoproterozoic displays distinct oscillatory zones.

DISCUSSION

Potential provenances to the Kuqa Subbasin and their geochronological constitution

First paleocurrent and depositional facies analysis had shown that all dominant clastic provenance sources for the Kuqa subbasin were from the Tian Shan and gradually migrated southward from Jurassic, through Cretaceous–Paleogene, to Neogene (Li *et al.*, 2004).

It should be pointed out that a widespread assemblage of medium-felsic volcanic rocks intrude within Carboniferous–Permian strata in the entire Tian Shan and within Silurian–Devonian strata in the South Tian Shan. We infer that Carboniferous–Permian strata from the south Tian Shan have been removed by erosion, exposing the large tract of Siliurian–Devonian strata in this area. However, the Yili–Central Tian Shan principally exposes abundant Carboniferous–Permian strata. Therefore, the early Paleozoic detrital zircons of the northern Kuqa Subbasin are likely derived from the South Tian Shan, although the late Paleozoic zircons could be derived from the both South Tian Shan and Yili–Central Tian Shan blocks.

In addition, two ophiolite belts and related crystalline rocks in the South Tian Shan yield SHRIMP U–Pb ages ranging between 452 and 640 Ma (Zhou *et al.*, 2004). Wang *et al.* (1998) also reported zircons from ophiolite samples on the top of high-pressure granulite terrane with U–Pb dates of ~440 Ma. Similar SHRIMP U–Pb ages (~425 Ma) were also obtained from zircons from basic gabbros at Kule lake, South Tian Shan (Long *et al.*, 2006). However Gao & Klemd (2003), Gao *et al.* (2006) presented numerous ages about 260–345 Ma, probably related to the late Paleozoic peak metamorphic and magmatic-thermal events between the South Tian Shan ocean and Yili–Central Tian Shan block.

Therefore, combined with investigating on the published U–Pb age data form the Tian Shan and Tarim blocks (Gao, 1990; Nakahjima *et al.*, 1990; Hu *et al.*, 1997, 2001; Wang *et al.*, 1998; Chen *et al.*, 1999a–c, 2000; Jiang *et al.*, 1999; Hu, 2000; Guo *et al.*, 2003; Han *et al.*, 2004; Liu *et al.*, 2004; Zhou *et al.*, 2004; Yang *et al.*, 2005, 2006; Zhang *et al.*, 2005; Long *et al.*, 2006, 2007; Gao *et al.*, 2006; Xu *et al.*, 2006; Zhu *et al.*, 2006), we found that there are notable geochronological differences among the Yili–Central Tian Shan, the South Tian Shan and the Tarim block, all potential provenance areas to the Kuqa Subbasin. The Yili–Central Tian Shan could supply the late Paleozoic zircons to the Kuqa Subbasin, and the South Tian Shan could supply detrital zircons of late Paleozoic, early Paleozoic and Proteozoic ages. However, those pre-Cambrian (esp. Archean) metamorphic zircons were early derived from the Tarim block, which most probably transported and deposited in the South Tian Shan ocean during Silurian–middle Devonian and/or late Devonian–Carboniferous time.

Detrital zircon geochronological implications for provenance changes

Based on the provenance geochronological considerations mentioned above, we contrast below the detrital zircon age spectra from the Kuqa Subbasin with those of potential provenance areas, discussing the implications for provenance and paleogeographical changes.

Detrital zircons of the Middle Jurassic sample mostly range from 370 to 450 Ma, with a small number of Proterozoic–Archean ages. This geochronological constitution is comparatively unimodal and indicates that the dominant source of detritus was likely from the northern South Tian Shan and southern Central Tian Shan (Figs 4a and 5), probably resulting from tectonic accretion events between the Yili–Central Tian Shan Block and the South Tian Shan Ocean that occurred during Silurian and early Devonian time, with dominant sandstone provenance tectonic attributes of passive continental margin discriminated by major element composition of whole-rock samples (Fig. 6).

The Lower Cretaceous sample shows a provenance with complicated detrital zircon age spectra, with new peak ages of 290–330 Ma as well as 370 (or 350)–450 Ma. We infer that these results reflect a new provenance supply produced by denudation of the South Tian Shan and South Tian Shan suture (Figs 4b and 5). These grains likely reflect Carboniferous–Permian volcanism and the Silurian–Devonian tectonic events between the South Tian Shan–Tarim and Yili–Central Tian Shan blocks, with dominant sandstone provenance tectonic attributes

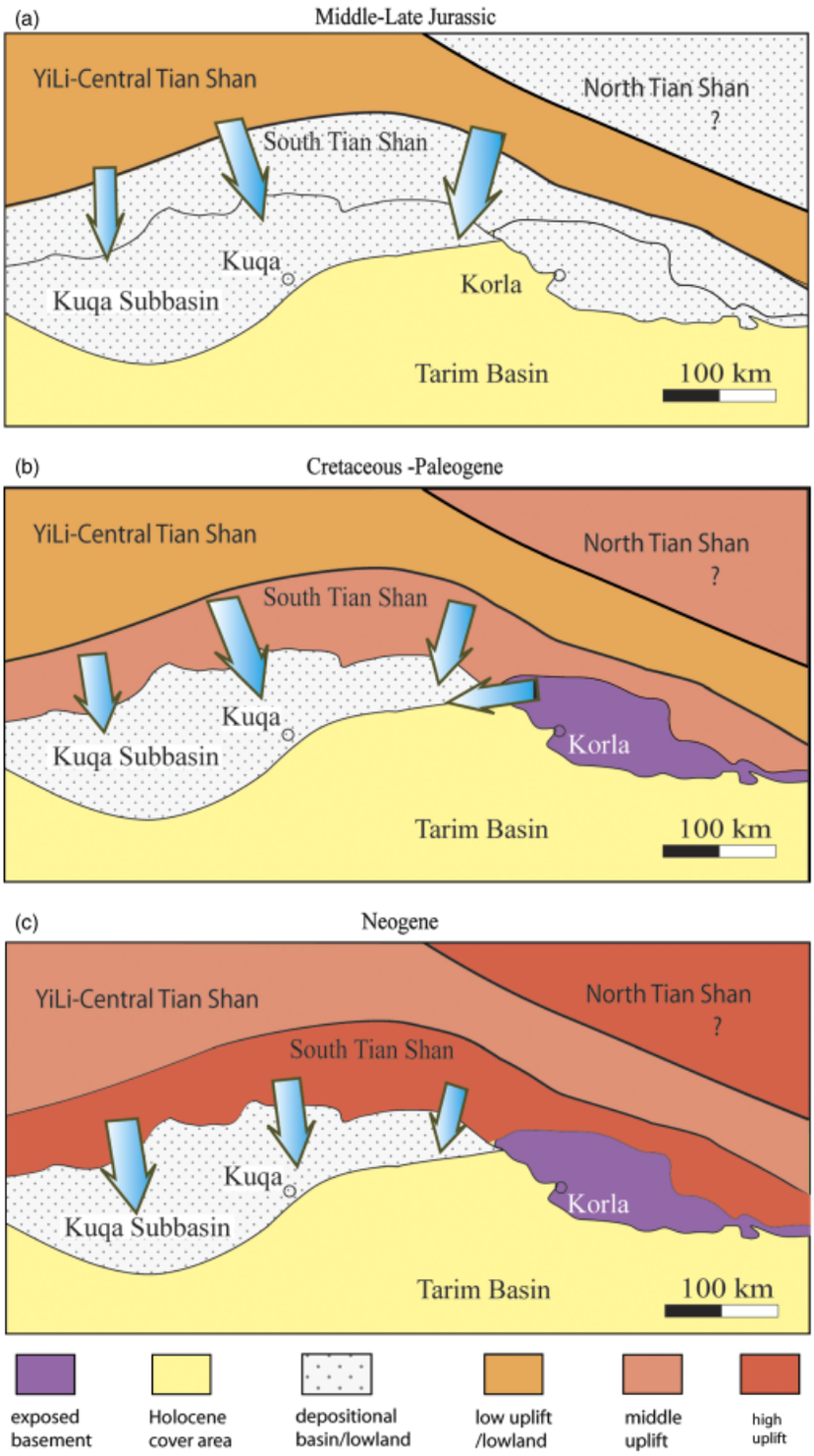

Fig. 4. Schematic map showing major provenance area changes from middle Jurassic (a), through Cretaceous–Paleogene (b), to Neogene (c). Arrowheads, with different width, indicate directions, power and ranges of major inferred provenance supply. Structural deformation and intracontinental shortening that occurred in the study area from Jurassic to Neogene is ignored on the above maps

of active continental margin or island arc (arc orogenic belt) (Fig. 6). In addition, several clusters of Proterozoic–Archean ages from this sample probably reflect that some provenance regions may have been deeply exhumated. The lack of obvious changes in detrital zircon age probability spectra between the Cretaceous and early Paleogene samples suggests that similar provenance types and basin-range framework likely continued from Cretaceous to early Paleogene time (Figs 4b and 5b).

In striking contrast to the Cretaceous and early Paleogene samples, detrital zircon age spectra from the Miocene sample display a relatively unimodal distribution, with peak age about 401–458 Ma older than the comparable provenance ages (peak ages about 370–450 Ma) of the Middle Jurassic and Lower Cretaceous samples. We infer that the major source of the Miocene sample was the southern South Tian Shan, with dominant sandstone provenance tectonic attributes

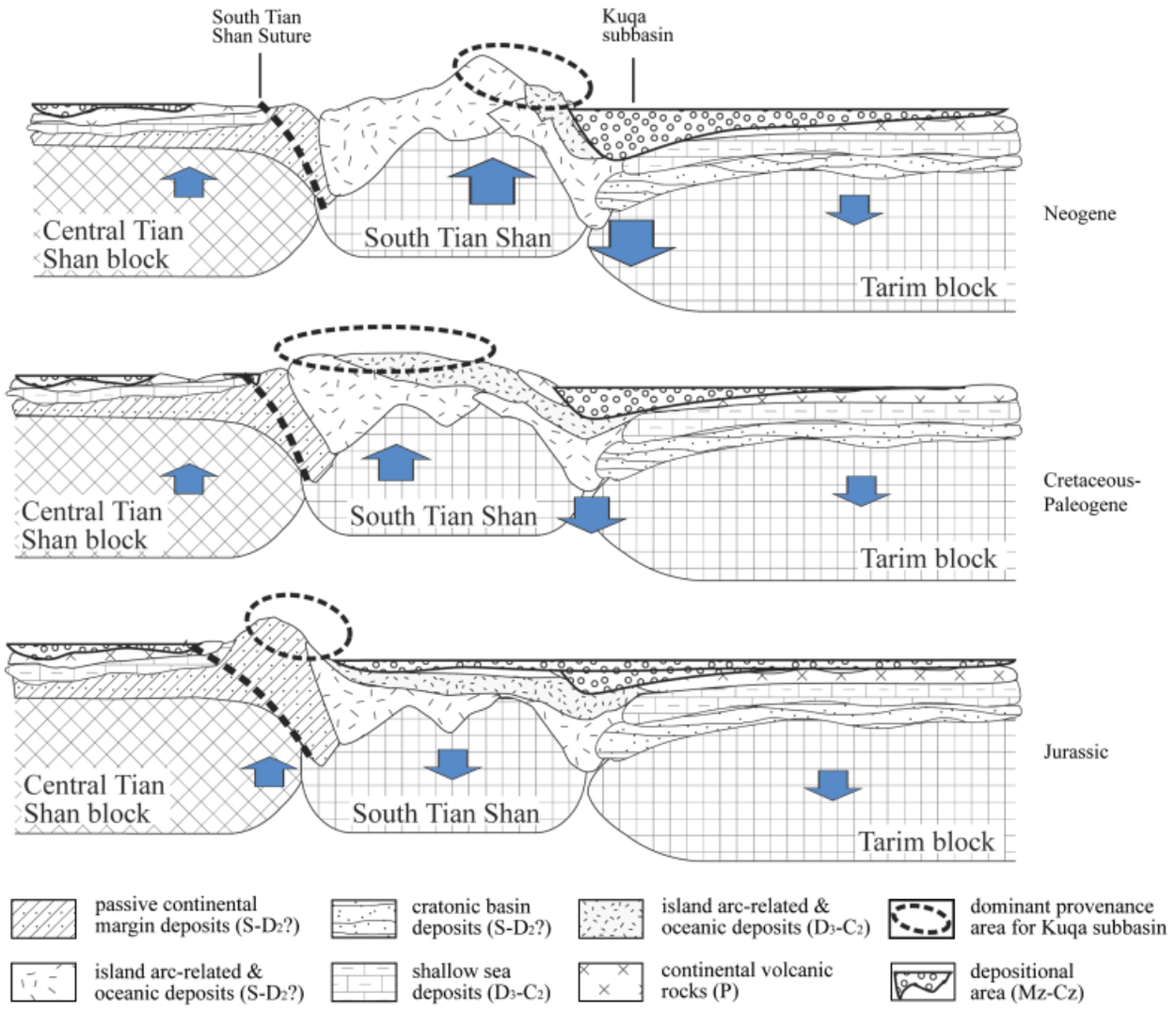

Fig. 5. Tectonic–stratigraphic profiles showing major provenance area changes from Jurassic, through Cretaceous–Paleogene, to Neogene time. Arrowheads indicate uplift or subsidence of the studied blocks. Structural deformation and intracontinental shortening that occurred in the study area from Jurassic to Neogene is ignored on the above profiles.

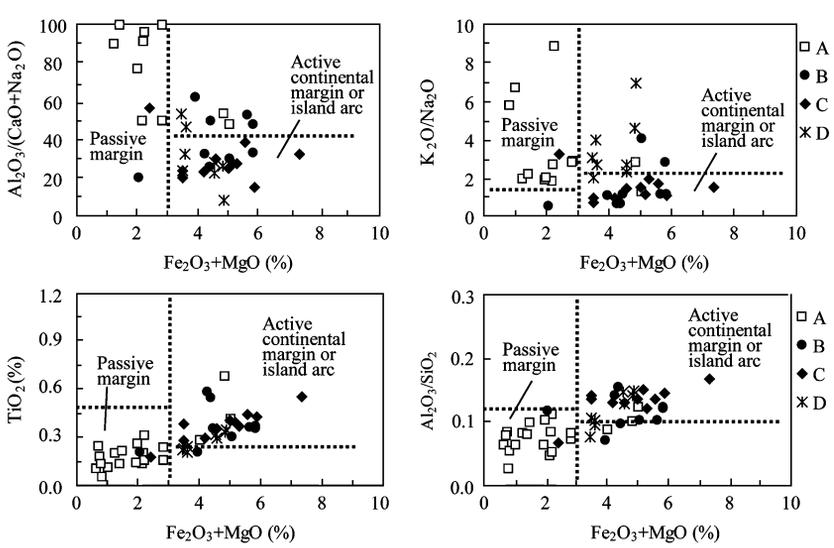

Fig. 6. Sandstone provenance tectonic attributes discriminated by major element composition of whole-rock samples of the Kuqa river profile, Kuqa subbasin. A, Jurassic samples; B, Cretaceous samples; C, Paleogene samples; D, Neogene samples. Data from Li *et al.* (2005).

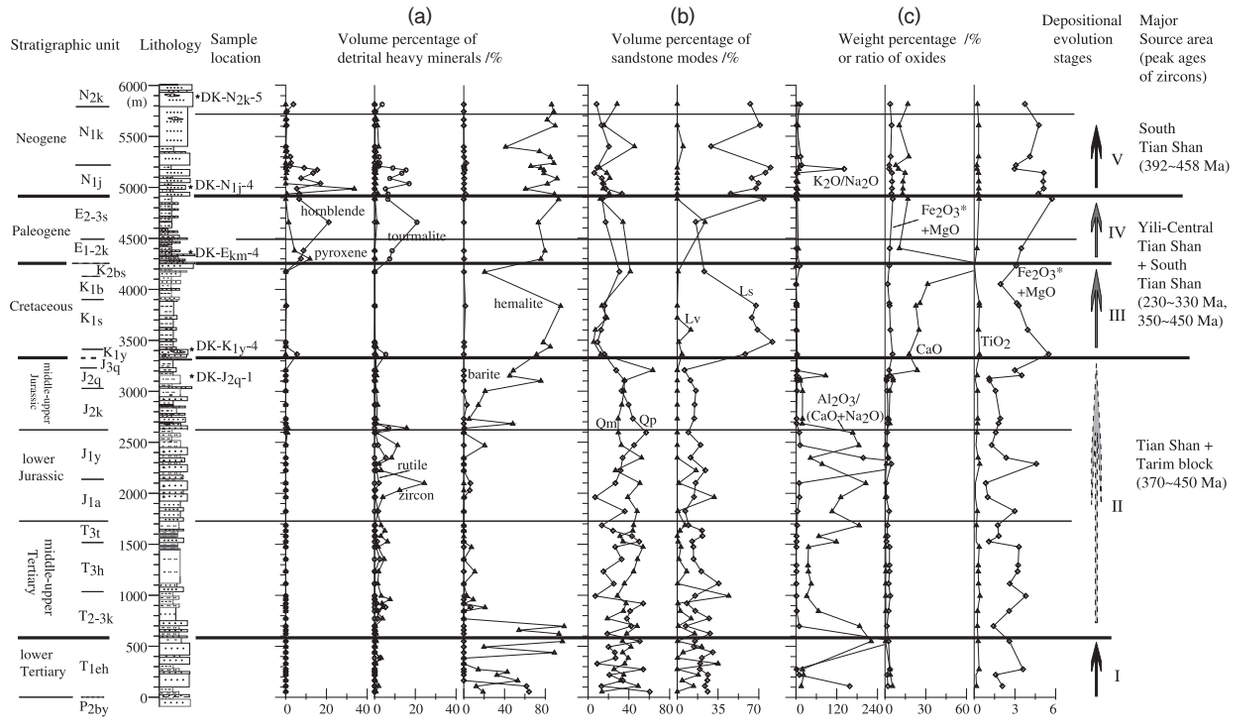

Fig. 7. Integrated depositional-geochemical records of the Kuqa river profile, Kuqa Subbasin. (a) Detrital heavy minerals; (b) sandstone modes: Qm, monocrystalline quartz; Qp, polycrystalline quartz; Lv, volcanic and metavolcanic lithic fragments; Ls, sedimentary and metasedimentary lithic fragments; (c) major element contents or their ratios of whole rocks. $Fe_2O_3^*$ means total iron as Fe_2O_3. I ~V indicate depositional evolutional stages (compiled and modified from Li *et al.*, 2004, 2005).

of active continental margin or island arc (arc orogenic belt) (Fig. 6). A similar age spectra was also found in the Pliocene sample (with peak age range of 392–456 Ma), suggesting that the southern South Tian Shan had become master clastic sources to Kuqa Subbasin since the Miocene epoch (Figs 4c and 5). Apparently intense uplift of the South Tian Shan (uplifting rate > denudation rate) resulted in source rocks from the South Tian Shan suture and Central Tian Shan belts becoming isolated from the Kuqa Subbasin by the highest peak area of the South Tian Shan.

Integrated depositional records responsive to basin-range interaction

Integrated analyses of the Mesozoic–Cenozoic depositional systems, sandstone framework grains, detrital heavy minerals and whole sandstones geochemical compositions from the Kuqa Subbasin (Li *et al.*, 2004, 2005) suggest that the depositional evolution in the Subbasin underwent five discontinuous phases. These phases are divided by four boundaries at Early Triassic\Middle Triassic, Middle–Late Jurassic\Early Cretaceous, Cretaceous\Paleogene and Paleogene\Neogene time (Fig. 7). These depositional systems and compositional changes reflect changes in the paleotectonic and paleogeographic settings in the Kuqa Subbasin–Tian Shan area (Li *et al.*, 2005). We infer that the first and second phase indicates a decreasing basin-range relief; and the latter phases reflect a gradually increasing relief, basically consistent with apatite fission track thermochronologic results presented by Dumitru *et al.* (2001).

U–Pb geochronological records of the five detrital zircon samples in this paper further provide detailed informations on the evolution of provenance and tectonic frameworks for the Kuqa Subbasin–Tian Shan basin-range system during late Mesozoic–Cenozoic time. Geochronological constitution of the Middle Jurassic sample reflects major provenances from the South Tian Shan even Yili–Central Tian Shan with gentle basin-range topography (Li *et al.*, 2005) under weak tectonic activity. The lower Cretaceous and early Paleogene samples reflect a new provenance supply resulting from intense denudation process of the South Tian Shan and the South Tian Shan suture with obvious basin-range topography (Li *et al.*, 2005). Finally the South Tian Shan became major provenances to Kuqa Subbasin since the Miocene time due to itself tectonic uplift that produced sharp basin-range topography (Li *et al.*, 2005) between the existent South Tian Shan and Kuqa Subbasin.

CONCLUSIONS

U–Pb geochronological records of the five detrital zircon samples from this paper provide detailed informations regarding provenance and tectonic evolution of the

Kuqa Subbasin–Tian Shan basin-range interaction during late Mesozoic through Neogene time. Geochronological constitution of the Middle Jurassic sample, 370–450 Ma with a small number of Proterozoic–Archean ages, reflects major provenances from the South Tian Shan even Yili–Central Tian Shan blocks with gentle basin-range topography under relatively quiescent tectonic conditions. Detrital zircon age spectra of the lower Cretaceous and lower Paleogene samples, dominated by grains ranging from 290 to 330 Ma as well as 370(or 350)–450 Ma with several clusters of Proterozoic ages, reflect a new provenance supply, resulting from intense denudation process of the South Tian Shan with rejuvenated basin-range topography. Finally the South Tian Shan, dominated by rocks of Silurian and Devonian age became the major source of the Kuqa Subbasin since the Miocene time due to itself tectonic uplift that resulted in sharp basin-range topography between the existent South Tian Shan and Kuqa Subbasin.

As a result of basin-range interaction between the Tian Shan and Kuqa Subbasin, the Jurassic–Neogene depositional records of the Kuqa Subbasin show distinct paleogeographic frameworks and three evolutionary stages. A relatively quiescent tectonic period during Jurassic time was characterized by broad drainage area and probably distant provenance area under decreasing basin-range relief. Active tectonism period in Cretaceous–Paleogene time resulting from intense uplift of the Tian Shan and basin-range differentiation produced a mixed provenance area from the South Tian Shan and Yili–Central Tian Shan under heated-dry climate.

ACKNOWLEDGEMENTS

The research was funded by the National Key Fundamental Research Project of China (Granted No. 2006CB202304), the National Natural Science Foundation Project of China (Granted No. 40472069) and the Key Frontier Project of Chinese Academy of Sciences (Granted No. KZCX3-SW-147). We wish to appreciate Profs. Liu Xiaoming, Ph.D. Diwu Chunrong and Lin Ciluan for their helpful to date zircons. We are also very grateful to Engineer Mao Qian and Ma Yuguang for their help on cathodoluminescence image analyses. Finally, many sincere thanks for two reviewers, Dr. Marc Hendrix and Dr. Edward Sobel, and the Basin Research editors (Dr. Alan Carroll *et al.*) for their valuable comments and revision suggestions on the manuscript.

REFERENCES

Allen, M.B, Vincent, S.J. & Wheeler, P.J. (1999) Late Cenozoic tectonics of the Kepingtage thrust zone: interpretation of the Tien Shan and Tarim Basin, Northwest China. *Tectonics*, **18**, 639–654.

Allen, M.F. & Zhang, C. (1992) Palaeozoic collisional tectonics and magmatism of the Chinese Tien Shan, Central Asia. *Tectonophysics*, **220**(1–4), 89–115.

Andersen, T. (2002) Correction of common lead in U–Pb analyses that do not report 204Pb. *Chem. Geol.*, **192**, 59–79.

Avouac, J.P., Tapponnier, P., Bai, M.H., You, H. & Wang, G. (1993) Active thrusting and folding along the northern Tianshan and late Cenozoic rotation of the Tarim relative to Dzungaria and Kazakhstan. *J. Geophys. Res.*, **98**(B4), 60755–60804.

Ballard, J.R., Palin, J.M., Williams, I.S., Campbell, I.H. & Faunes, A. (2001) Two-ages of porphyry intrusion resolved for the super-giant Chuquicamata copper deposit of northern Chile by ELA-ICP-MS and SHRIMP. *Geology*, **29**, 383–386.

Burtman, V.S. (2000) Cenozoic crustal shortening between the Pamir and Tien Shan and a reconstruction of the Pamir-Tien Shan transition zone for the Cretaceous and Paleogene. *Tectonophysics*, **319**, 69–92.

Burtman, V.S., Skobelev, S.F. & Molnar, P. (1996) Late Cenozoic slip on the Talas-Ferghana fault, the Tian Shan, Central Asia. *Geol. Soc. Am. Bull.*, **108**, 1004–1021.

Carroll, A.R., Graham, S.A. & Hendrix, M.S. (1995) Late Paleozoic tectonic amalgamation of northwestern China: sedimentary record of the northern Tarim, northwestern Turpan and southern Junggar basins. *Geol. Soc. Am. Bull.*, **107**, 571–594.

Carroll, A.R., Liang, Y., Graham, S.A., Hendrix, M.S, Ying, D. & Zhou, D. (1990) Junggar basin,northwest China, Trapped late Paleozoic ocean. *Tectonophysics*, **181**, 1–14.

Chen, Ch.M., Lu, H.F. & Dong, J. (1999a) Closing history of the southern Tianshan oceanic basin, western China: an oblique collisional orogeny. *Tectonophysics*, **302**, 23–40.

Chen, Y.B., Hu, A.Q., Zhang, G.X. & Zhang, Q.F. (1999b) Zircon U Pb geochronology of granitic gneiss at Du-ku Highway of Southwestern Tianshan and its implications. *Chin. Sci. Bull.*, **44**(21), 2328–2332 (in Chinese with English abstract).

Chen, Y.B., Hu, A.Q., Zhang, G.X. & Zhang, Q.F. (1999c) Zircon U-Pb age and Nd-Sr isotopic composition of granitic gneiss and its geological implications from Precambrian window of western Tianshan, NW China. *Geochimica*, **28**(6), 515–520 (in Chinese with English abstract).

Chen, Y.B., Hu, A.Q., Zhang, G.X. & Zhang, Q.F. (2000) Precambrian basement age and characteristics of Southwestern Tianshan: Zircon U Pb geochronology and Nd Sr isotopic compositions. *Acta Petrol. Sin.*, **16**(1), 92–98 (in Chinese with English abstract).

Coleman, R.G. (1989) Contiental growth of Northwest China. *Tectonics*, **8**, 621–635.

Dewey, J.F., Shackleton, R. & Chang, C. (1988) The Tectonic evolution of the Tibetian Plateau. *Phil. Trans. R. Soc. Lond.*, **A327**, 379–413.

Dumitru, T.A., Zhou, D., Chang, E., Graham, S.A., Hendrix, M.S., Sobel, E.R. & Carroll, A.R. (2001) Uplift, exhumation and deformation in the Chinese Tian Shan. In: *Paleozoic and Mesozoic Tectonic Evolution of Central and Eastern Asia: From Continental Assembly to Intracontinental Deformation* (Ed. by M.S. Hendrix & G.A. Davis, *Geol. Soc. Am. Mem.*, **194**, 71–99.

Gao, J. & Klemd, R. (2003) Formation of HP-LT rocks and their tectonic implications in the western Tianshan Orogen, NW China: geochemical and age constraints. *Lithos*, **66**, 1–22.

Gao, J., Li, M.S., Xiao, X.C., Tang, Y.H. & Guo, Q. (1998) Paleozoic tectonic evolution of the Tianshan Orogen, northwest China. *Tectonophysicas*, **287**, 213–231.

Gao, J., Long, L.L., Qian, Q., Su, W. & Klemd, R. (2006) South Tianshan: a Late Paleozoic or a Triassic orogen? *Acta Petrol. Sin.*, **22**(5), 1049–1061 (in Chinese with English abstract).

Gao, Z. (1990) Further discussion on the problem of the Precambrian stratigraphy in Tianshan area. *Xinjiang Geol.*, **8**(1), 80–90 (in Chinese with English abstract).

Graham, S.A, Hendrix, M.S., Wang, L.B. & Carroll, A.R. (1993) Collisional successor basins of western China: impact of tctonic inheritance on sand composition. *Geol. Soc. Am. Bull.*, **105**, 323–344.

Guo, Z.J., Zhang, Z.C., Liu, S.W. & Li, H.M. (2003) U-Pb geochronological evidence for the early Precambrian complex of the Tarim Craton, NW China. *Acta Petrol. Sin.*, **19**(3), 537–542 (in Chinese with English abstract).

Han, B.F., He, G.Q., Wu, T.R. & Li, H.M. (2004) Zircon U-Pb dating and geochemical features of early paleozoic granites from Tianshan,Xinjiang: implications for tectonic evolution. *Xinjiang Geol.*, **22**(1), 3–11 (in Chinese with English abstract).

Heermance, R.V., Chen, J., Burbank, D.W. & Wang, C.S. (2007) Chronology and tectonic controls of Late Tertiary deposition in the southwestern Tian Shan foreland, NW China. *Basin Res.*, **19**(4), 599–632.

Hendrix, M.S. (2000) Evolution of Mesozoic sandstone compositions, southern Junggar, northern Tarim, and western Turpan basins, Northwest China: a detrital record of the ancestral Tian Shan. *J. Sediment. Res.*, **70**(3), 520–532.

Hendrix, M.S., Graham, S.A., Carroll, A.R., Sober, E.R., Mcknight, C.L., Shulein, B.J. & Wang, Z.X. (1992) Sedimentary record and climatic implication of recurrent deformation of the Tien Shan: evidence from Mesozoic strata of the north Tarim, south Junggar and Turpan basins. *Geol. Soc. Am. Bull.*, **104**, 53–79.

Hu, A.Q. (2000) Crustal evolution and Phanerozoic crustal growth in northern Xinjiang: Nd isotopic evidence Part I: isotopic characterization of basement rocks. *Tectonophysics*, **328**, 15–51.

Hu, A.Q.,Wang, Zh.G. & Tu, G.Zh. (1997) *The Geologic Evolution and Diagenetic-metallogenic Rule in the Northern Xinjiang*. China Science Press, Beijing (in Chinese).

Hu, A.Q., Zhang, G.X., Chen, Y.B. & Zhang, Q.F. (2001) A model of division of the continental Crus basement and the time scales of the major geological events in the Xinjiang-based on studies of isotopic geochronology and geochemistry. *Xinjiang Geol.*, **19**(1), 12–19 (in Chinese with English abstract).

Jia, C. (1997) *Structure and Oil-Gas in Tarim Basin, China*. Petroleum Industry Press, Beijing, 348–364 (in Chinese with English abstract).

Jiang, Ch.Y., Mu, Y.M., Bai, K.Y., Zhao, X.N., Zhang, H.B. & Hei, A.Z. (1999) Chronology, petrology, geochemistry and tectonic environment of granitoids in the southern Tianshan Mountain, western China. *Acta Petrol. Sin.*, **5**(2), 298–308 (in Chinese with English abstract).

Li, Z., Guo, H., Wang, D.X. & Lin, W. (2005) Mesozoic-Cenozoic tectonic transition in Kuqa Depression-Tianshan, Northwest China: evidence from Sandstone Detrital and Geochemical Records. *Sci. China (Ser. D)*, **48**(9), 1387–1402.

Li, Z., Song, W.J., Peng, S.T., Wang, D.X. & Zhang, Z.P. (2004) Mesozoic–Cenozoic tectonic relationships between the Kuqa Subbasin and Tian Shan, northwest China: constraints from depositional records. *Sediment. Geol.*, **172**, 223–249.

Li, Z., Wang, Q., Wang, D., Lin, W. & Wang, Q.C. (2003) Depositional record constraints on Late Cenozoic uplift of Tian Shan and tectonic transformation in Kuqa Subbasin, West China. *Acta Sedimentol. Sin.*, **21**(1), 38–45 (in Chinese with English abstract).

Liu, C.X., Xu, B.L., Zu, T.R., Lu, F.X., Tong, Y. & Cai, J.H. (2004) Petrochemistry and tectonic significance of Hercynian Alkaline rocks along the Northern margin of the Tarim platform and its adjacent area. *Xinjiang Geol.*, **22**(1), 43–49 (in Chinese with English abstract).

Liu, H., Wang, Z., Xiong, B., Li, Y., Liu, L.M. & Zhang, J. (2000) Coupling analysis of Mesozoic-Cenozoic foreland basin and mountain system in central and western China. *Earth Sci. Front.*, **7**(3), 55–72 (in Chinese with English abstract).

Long, L.L., Gao, J., Xiong, X.M. & Qian, Q. (2006) The geochemical characteristics and the age of the Kule Lake ophiolite in the southern Tianshan. *Acta Petrol. Sin.*, **22**(1), 65–73 (in Chinese with English abstract).

Long, L.L., Gao, J., Xiong, X.M. & Qian, Q. (2007) Geochemistry and geochronology of granitoids in Bikai region, southern Central-Tianshan mountains, Xinjiang. *Acta Petrol. Sin.*, **23**(4), 719–732 (in Chinese with English abstract).

Lu, H., Howell, D.G. & Jia, D. (1994) Rejuvenation of the Kuqa foreland basin, northern flank of the Tarim basin, northwest China. *Int. Geol. Rev.*, **36**, 1151–1158.

Ludwig, K.R. (2003) ISOPLOT 3.0: a geochronological toolkit for Microsoft Excel, Berkeley Geochronology Center. Spec. Pub., 4.

Molnar, P. & Tapponier, P. (1975) Cenozoic tectonics of Asia: effects of a continental collision. *Science*, **189**(4201), 419–426.

Nakahjima, T., Uchiumi, S., Maruyama, S., Liou, J.G. & Wang, X. (1990) Evidence for late Proterozoic subduction from 700-Mya-old blueschist in China. *Nature*, **346**, 263–265.

Sengör, A.M.C., Natal'in, B.A. & Burtman, V.S. (1993) Evolution of the Altaid tectonic collage and Paleozoic crustal growth in Eurasia. *Nature*, **364**, 299–307.

Sircombe, K.N. (1999) Tracing provenance through the isotope ages of littoral and sedimentary detrital zircon, eastern Australia. *Sediment. Geol.*, **124**, 47–67.

Tapponier, P. & Molnar, P. (1979) Active faulting and Cenozoic tectonics of the Tian Shan, Mongolia and Baykal regions. *J. Geophys. Res.*, **84**, 3425–3459.

Wang, R.S., Wang, Y. & Li, H.M. (1998) Zircon U-Pb age and its geological significance of high-pressure terrane of granulite facies in Yushugou area, Southern Tianshan Mountain. *Geochimica*, **27**(6), 522–527 (in Chinese with English abstract).

Wiedenbeck, M., Alle, P., Corfu, F., Griffin, W.L., Meier, F., Oberli, F., Von Quadt, A., Roddick, J.C. & Spiegel, W. (1995) Three natural zircon standards for U–Th–Pb, Lu–Hf, trace element, and REE analyses. *Geostand. Newslett.*, **19**, 1–23.

Windley, B.F., Alexeiev, D., Xiao, W., Kroner, A. & Badarch, G. (2007) Tectonic models for accretion of the Central Asian Orogenic Belt. *J. Geol. Soc., Lond.*, **164**, 31–47.

Windley, B.F., Allen, M.B., Zhang, C., Zhao, Z. & Wang, Q. (1990) Paleozoic accretion and Cenozoic redeformation of the Chinese Tien shan Ranges, central Asia. *Geology*, **18**, 128–131.

Xu, X.Y., Ma, Zh.P., Xia, Z.Ch., Li, X.M. & Wang, L.S. (2006) TIMS U-Pb isotopic dating and geochemical characteristics of Paleozoic Granitic rocks from the Middle-Western Section of Tianshan. *Northwestern Geol.*, **39**(1), 50–57 (in Chinese with English abstract).

Yang, H.B., Gao, P., Li, B. & Zhang, Q.J. (2005) The geological character og thr Sinian Dalubayyi Ophioianshan. *Xinjiang. Xinjiang Geol.*, **23**(2), 123–126. (in Chinese with English abstract).

Yang, T.N., Li, J.Y., Sun, G.H. & Wang, Y.B. (2006) Earlier Devonian acticve continental arc in Central Tianshan: evidence of geochemical analyses and zircom SHRIMP dating on mylonitized granitic rock. *Acta Petrol. Sin.*, **22**(1), 41–48 (in Chinese with English abstract).

Yin, A., Nie, S., Craig, P., Harrison, T.M., Ryerson, F.J., Qian, X. & Yang, G. (1998) Late Cenozoic tectonic evolution of the southern Chinese Tian Shan. *Tectonics*, **17**(1), 1–27.

Yuan, H.L., Gao, S. & Liu, X.M. (2004) Accurate U-Pb age and trace element determinations of zircon by laser ablation-inductively coupled plasma mass spectrometry. *Geoanal. Geostand. Res.*, **28**(3), 353–370.

Zhang, L.F., Ai, Y.L., Li, Q., Li, X.P., Song, X.G. & Wei, C.J. (2005) The formation and tectonic evolution of UHP metamorphic belt in southwestern Tianshan, Xinjiang. *Acta Petrol. Sin.*, **21**(4), 1029–1038 (in Chinese with English abstract).

Zhou, D., Graham, S.A., Chang, E.Z., Wang, B. & Hacker, B. (2001) Paleozoic tectonic amalgamation of the Chinese Tian Shan: evidence from a transect along the Dushanzi-Kuqa Highway. In: *Paleozoic and Mesozoic Tectonic Evolution of Central and Eastern Asia: From Continental Assembly to Intracontinental Deformation* (Ed. by M.S. Hendrix & G.A. Davis, *Geol. Soc. Am. Mem.*, **194**, 23–46.

Zhou, D.W., Su, L. & Jian, P. (2004) Zircon U-Pb SHRIMP ages of high-pressure granulite in Yushugou ophiolitic terrane in southern Tianshan and their tectonic implications. *Chin. Sci. Bull.*, **13**, 1411–1415 (in Chinese with English abstract).

Zhu, Z.X., Wang, K.Zh., Zheng, Y.J., Sun, G.H., Zhang, C. & Li, Y.P. (2006) Zircon SHRIMP dating of Silurian and Devonian granitic intrusions in the southern Yili block, Xinjiang and preliminary discussion on their tectonic setting. *Acta Petrol. Sin.*, **22**(5), 1193–1200 (in Chinese with English abstract).

Supporting Information

Additional Supporting Information may be found in the online version of this article:

Appendix S1. U-Pb Geochronologic analysis of detrital zircons from the Kuqa Formation (N_{2k}) sandstone sample.

Appendix S2. U-Pb Geochronologic analysis of detrital zircons from the Jidike Formation (N_{1j}) sandstone sample.

Appendix S3. U-Pb Geochronologic analysis of detrital zircons from the Kumugeliemu Formation (E_{km}) sandstone sample.

Appendix S4. U-Pb Geochronologic analysis of detrital zircons from the Yageliemu Formation (K_{1y}) sandstone sample.

Appendix S5. U-Pb Geochronologic analysis of detrital zircons from the Qiakemake Formation (J_{2q}) sandstone sample.

Please note: Wiley-Blackwell are not responsible for the content or functionality of any supporting materials supplied by the authors. Any queries (other than missing material) should be directed to the corresponding author for the article.

Manuscript received 7 April 2009; Manuscript accepted 13 August 2009.

